

Investigations on Caesium-free Alternatives for H⁻ Formation at Ion Source Relevant Parameters

U. Kurutz*,† and U. Fantz*,†

*Max-Planck-Institut für Plasmaphysik, Boltzmannstr. 2, 85748 Garching, Germany
†AG Experimentelle Plasmaphysik, Institut für Physik, Universität Augsburg, 86135 Augsburg, Germany

Abstract. Negative hydrogen ions are efficiently produced in ion sources by the application of caesium. Due to a thereby induced lowering of the work function of a converter surface a direct conversion of impinging hydrogen atoms and positive ions into negative ions is maintained. However, due to the complex caesium chemistry and dynamics a long-term behaviour is inherent for the application of caesium that affects the stability and reliability of negative ion sources. To overcome these drawbacks caesium-free alternatives for efficient negative ion formation are investigated at the flexible laboratory setup HOMER (HOMogenous Electron cyclotron Resonance plasma). By the usage of a meshed grid the tandem principle is applied allowing for investigations on material induced negative ion formation under plasma parameters relevant for ion source operation. The effect of different sample materials on the ratio of the negative ion density to the electron density n_{H^-}/n_e is compared to the effect of a stainless steel reference sample and investigated by means of laser photodetachment in a pressure range from 0.3 to 3 Pa. For the stainless steel sample no surface induced effect on the negative ion density is present and the measured negative ion densities are resulting from pure volume formation and destruction processes. In a first step the dependency of n_{H^-}/n_e on the sample distance has been investigated for a caesiated stainless steel sample. At a distance of 0.5 cm at 0.3 Pa the density ratio is 3 times enhanced compared to the reference sample confirming the surface production of negative ions. In contrast for the caesium-free material samples, tantalum and tungsten, the same dependency on pressure and distance n_{H^-}/n_e like for the stainless steel reference sample were obtained within the error margins: A density ratio of around 14.5% is measured at 4.5 cm sample distance and 0.3 Pa, linearly decreasing with decreasing distance to 7% at 1.5 cm. Thus, tantalum and tungsten do not significantly affect the negative ion density. First measurements conducted with LaB₆ as well as with two types of diamond like carbon (DLC) n_{H^-}/n_e of about 15% at 1 Pa were measured, which is comparable to the density ratio obtained for the stainless steel reference sample. At HOMER a surface induced enhancement of n_{H^-} is only observed when it exceeds the volume formation of H⁻ which is also realistic for negative hydrogen ion sources.

INTRODUCTION

An efficient way of negative ion formation in negative hydrogen ion sources is based on the surface conversion process where the negative ion formation probability is strongly enhanced by the application of caesium. The underlying principle is the reduction of a converter surfaces work function enabling a direct conversion of impinging hydrogen neutrals and positive ions into negative ions [1, 2]. As generally known this method is capable of providing high amounts of extracted negative ions and simultaneously low co-extracted electrons. For the neutral beam injection (NBI) in fusion research, the strict requirements of high negative ion current densities and a low amount of co-extracted electrons at an operation pressure of 0.3 Pa can presently only be fulfilled by the application of caesium [3].

However, there are several drawbacks for ion source operation inherent to the usage of caesium. As a consequence of the complex caesium chemistry and its dynamic long-term behaviour specific maintenance routines such as caesium-conditioning are required and the long-term stability and reliability is affected [4]. The formation of caesium compounds with background impurities leads to an increase of the work function followed by a decreased negative ion formation efficiency and an enhancement of co-extracted electrons. Hence frequent evaporation of fresh caesium is necessary giving rise to the issue of an increased caesium consumption. To overcome these drawbacks, alternative materials for efficient negative ion formation in ion sources are highly desired.

Numerous investigations on materials suitable for H⁻ formation at a material surface or close to it are present focusing on various applications and are performed within a wide range of fields and parameters [5–14]. For example have tantalum and tungsten revealed an enhancing effect on highly vibrationally excited hydrogen molecules H₂(X,v') in gas phase experiments [15–17]. As this is beneficial for the volume production of negative ions via dissociative attachment (H₂(X,v'') + e⁻ → H⁻ + H) the effect of tantalum has been investigated at the volume source Camembert III where elevated negative ion densities have been observed [11]. On the contrary at the H⁻ test stand at CEA Saclay the

extracted H⁻ current diminished in combination with tantalum [18]. For different graphites e.g. diamond like carbon (DLC) negative ion yields have been measured in beam experiments [7, 19] and in low-pressure hydrogen plasmas with low electron density ($n_e \sim 10^{14} \text{ m}^{-3}$) and high electron temperatures ($T_e \sim 5 - 6 \text{ eV}$) [14]. In the latter experimental setup negative ion formation has been reported due to DLC, highly ordered pyrolytic graphites (HOPG) and boron doped diamond (BDD) showing a dependency of the H⁻ yield on the sample temperature which is related to a variation in the sp³/sp² hybridisation ratio [13, 14, 20]. Furthermore utilizing the pure surface production of H⁻ at materials with inherent low work function like LaB₆ or BaO may also be suitable for an application at ion sources.

Although capable to form negative ions in the dedicated experiments described in the literature the suitability of such materials for the application in negative hydrogen ion sources is not ensured. Therefore direct comparable measurements at ion source relevant parameters are mandatory.

These investigations are performed in hydrogen and deuterium at the cw-driven ECR-discharge HOMER (HOMogenous electron cyclotron Resonance plasma) where plasma parameters of $10^{16} \text{ m}^{-3} \leq n_e \leq 10^{17} \text{ m}^{-3}$, T_e in the range of 1 – 2 eV and atomic densities n_H between 10^{18} m^{-3} and 10^{19} m^{-3} are present in a pressure range from 0.3 to 3 Pa. The effect of different sample materials on the negative ion density is measured by means of laser photodetachment and investigations on the influence of the samples potential and temperature as well as locally resolved negative ion density profiles as a function of the sample distance are performed.

EXPERIMENTAL SETUP

The experimental setup of the ECR-discharge HOMER is shown in figure 1. The cylindrical vacuum vessel is made of stainless steel having a diameter of 15 cm and a total height of 31 cm. An axial magnetic field of 87.5 mT needed for resonant electron cyclotron heating at 2.45 GHz is produced homogeneously over the whole volume by two water cooled coils located at the top and the bottom part of the vessel. The microwave induced through a borosilicate glass plate from the top of the vessel has a maximum power output of 1 kW. The vacuum system allows for operation down to a pressure of 0.3 Pa at a gas flow of 9 sccm. At HOMER the tandem principle is applied using the meshed grid method as an alternative to a magnetic filter field [21]. The meshed grid is made of stainless steel (mesh size 1 mm) and is located in a distance of 12 cm from the top of the vessel. The grid potential can be biased relative to the grounded walls or set to be floating allowing for influencing the diffusion of charged particles through the grid.

In the diffusive downstream region beneath the meshed grid a horizontal oriented sample holder of 8.5x6 cm² made of stainless steel is located. The sample holder is thermally and electrically insulated and its axial position is variable. Samples can be heated up to 800 °C via heating elements inside the sample holder and the temperature is monitored by a thermo-couple. The sample holder bias can be modified relative to the grounded walls or the meshed grid affecting the energy of charged particles impinging on the investigated samples.

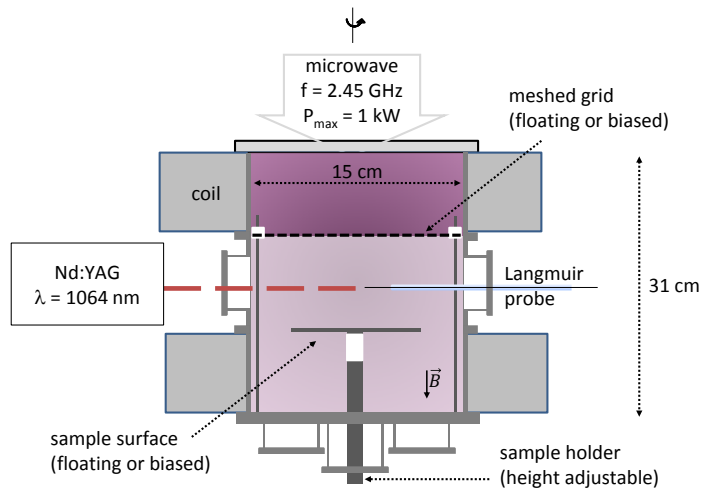


FIGURE 1. Schematic of the experimental setup of the ECR-discharge HOMER.

Diagnostics

The negative ion density in the downstream plasma region beneath the meshed grid is measured locally by means of laser photodetachment [22]. Based on the photodetachment process ($H^- + h\nu \rightarrow H + e$) a short laser pulse is injected into the plasma to destroy all negative hydrogen ions within the laser beam. The laser is adjusted to the tip of a Langmuir probe that is biased above the plasma potential. Without laser pulse the current measured by the Langmuir probe I_0 is solely carried by electrons hence proportional to n_e whereas due to the injected laser pulse a sharp increase in the measured electron current ΔI proportional to n_{H^-} is obtained. The ratio of the increased signal amplitude ΔI to I_0 determines the density ratio of negative ions to the electron density n_{H^-}/n_e . Absolute values of n_{H^-} can be derived by multiplication of the relative negative ion density n_{H^-}/n_e with the electron density independently determined by the Langmuir probe. However, uncertainties related to the measurement of n_e affect the error margin of obtained absolute negative ion densities.

For the laser photodetachment system at HOMER a Nd:YAG laser ($\lambda = 1064$ nm, beam diameter 6 mm) is used, axially aligned to the probe tip. Per 8 ns pulse typically 22.5 mJ pulse energy (photodetachment efficiency $\geq 99.99\%$) are applied. The Langmuir probe is biased at 35 V ($\phi_{pl} \leq 5$ V). Due to inherent variations of the microwave power output n_e oscillates on a microseconds time scale. In order to guarantee that measurements are performed at comparable plasma parameters i.e. electron densities a rapid-triggering circuit is used that triggers the laser on the set value of the electron current. The error margin for n_{H^-}/n_e due to statistical deviations is typically in the order of 15%. The reliability of the applied laser photodetachment system has been successfully benchmarked against high reliable but line of sight integrated cavity ring-down spectroscopy [23]. Profiles of the negative ion density are determined as a function of distance to the sample surface by height variations of the sample holder keeping the position of the laser photodetachment system fixed. Although the plasma is influenced by this method, it comprises the advantage of a high flexibility while maintaining permanent adjustment of the laser beam centred to the probe tip. Measurements on the effect of different material samples on the negative ion density are always compared to ones performed with a stainless steel reference sample. Therefore, the impact on the plasma by an adjustment of the sample holders' axial position is comparable for the respective measurements.

The electron density and further plasma parameters are determined by means of Langmuir probe and optical emission spectroscopy (OES). Due to the presence of the magnetic field n_e is deduced by measuring the positive ion density $n_{H_x^+}$ ($x=1,2,3$) using the orbital-motion-limited theory and applying the quasi neutrality $n_e = \sum_{x=1}^3 n_{H_x^+} - n_{H^-}$. For deducing n_e the negative ion density has to be taken into account as long as n_{H^-}/n_e is exceeding the error margin of determining $n_{H_x^+}$ namely $\geq 20\%$.

While $n_{H_x^+} \approx n_e$, ϕ_{pl} , ϕ_{fl} and T_e are obtained by Langmuir probe measurements, OES is used for deducing the density ratio of atomic to molecular hydrogen n_H/n_{H_2} as well as the vibrational and rotational population of $H_2(X,v)$. By the assumption of a Boltzmann distribution for the population of the low vibrational states ($v \leq 4$) a vibrational temperature T_{vib} and for the rotational population the gas temperature T_{gas} is obtained [24]. Furthermore, 0-dimensional modelling of the volume processes for negative ions is used assisting the interpretation of measured negative ion densities [23]. In this model volume production via dissociative attachment is balanced against the destruction via electron detachment, (non-)associative detachment due to atomic hydrogen collisions and mutual neutralisation due to positive ion collisions.

Influence of the meshed grid

Investigating the effect of the meshed grid on the volume formation and destruction mechanisms of negative ions has been performed with the reference stainless steel sample.

The influence of the floating meshed grid on the positive ion density over the pressure range from 0.3 to 3 Pa at a discharge power of 300 W is displayed in figure 2(a). By the meshed grid the positive ion density is decreased over the whole pressure range by a factor of 3 showing a maximum at 1 Pa. In the presence of the meshed grid n_{H^-}/n_e is above 10% and is decreased below 5% without the meshed grid whereas the dependence on the pressure changes, too. Thus, virtually the same n_{H^-} with reduced n_e is obtained verifying that the tandem principle is accomplished by the meshed grid.

According to the tandem principle vibrationally excited hydrogen molecules formed in the source region above the meshed grid diffuse into the downstream region where negative ions are formed via dissociative attachment. However, the measured reduced electron density in this diffusive downstream region has a diminishing effect on the rate of

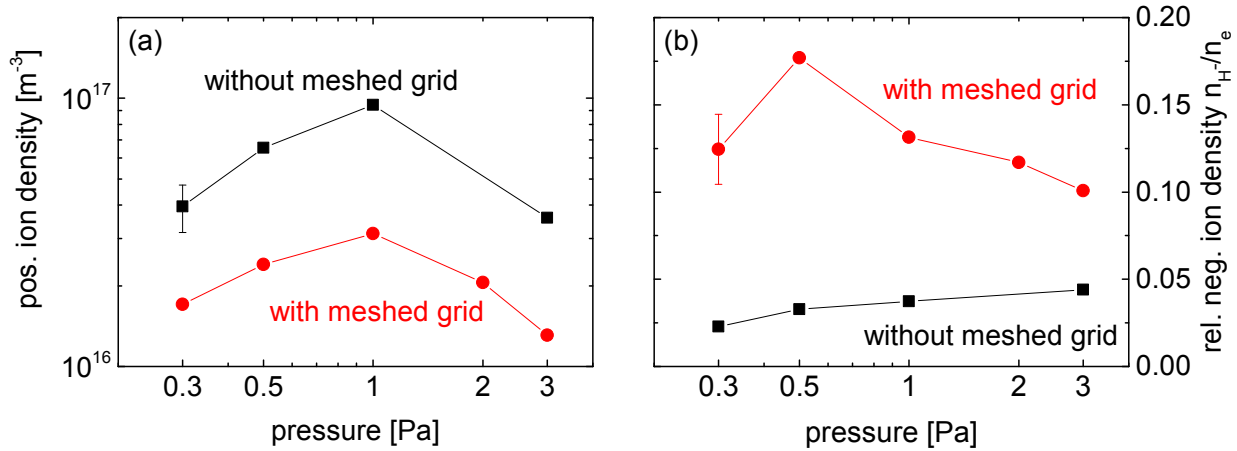


FIGURE 2. Influence of the floating meshed grid at 300 W discharge power (a) on the positive ion density and (b) on the relative negative ion density.

volume production of n_{H}^- . On the contrary, the destruction rates by electron detachment and mutual neutralisation due to collisions with positive ions is also decreased. As in the downstream of the meshed grid moreover a reduced atomic hydrogen density has been measured by OES, the destruction of H^- due to collisions with atoms additionally is reduced. In consequence, by the application of the tandem principle using the meshed grid, virtually the same n_{H}^- values are obtained with significant increased n_{H}^-/n_e and thus a better signal-to-noise ratio.

RESULTS

The effect of surfaces made of tantalum, tungsten, LaB_6 and two types of DLC as well as a caesiated stainless steel sample on the negative ion density is investigated. For tantalum and tungsten an enhanced volume production of negative ions is expected whereas for LaB_6 , DLC and the caesiated stainless steel sample a direct surface production of negative ions should be the underlying mechanism.

The size of the samples made of tantalum, tungsten and DLC is $8.5 \times 6 \text{ cm}^2$, the size of the caesiated steel and LaB_6 samples $3 \times 3 \text{ cm}^2$. In the case of tantalum and tungsten the samples have been prepared by polishing and chemically cleaning in an ultra-sonic bath with acetone and isopropyl. The caesiated stainless steel sample has been prepared at the test bed ACCesS [25] and transferred to HOMER afterwards. The application of caesium at ACCesS has been maintained by evaporation of caesium onto a polished stainless steel sample. A work function of 3 eV after the caesiation in vacuum [25] and a degraded work function of 3.3 eV after atmospheric pressure exposure has been measured in ACCesS. No mechanical and chemical cleaning has been applied on the LaB_6 and DLC samples in order not to manipulate the surface structure. The polycrystalline LaB_6 sample has been cleaned by heating the sample up to 300 °C in vacuum at HOMER for 48 hours. The DLC samples are of $2.5 - 3 \mu\text{m}$ thickness and differ in their surface roughness in order to investigate this effect on the negative ion formation. The hydrogen content of these amorphous DLC samples that are manufactured by PVD-sputtering is in the range of 20%. No additional cleaning procedure has been applied on these two DLC samples.

Variation of sample distance and hydrogen pressure

The measured density ratio of negative ions to electrons n_{H}^-/n_e for tantalum, tungsten and the caesiated stainless steel samples is compared to the stainless steel reference sample and presented in figure 3. The relative negative ion densities are measured for the samples at floating potential as (a) a function of distance from the sample at 0.3 Pa for all samples and (b) as a function of pressure at a distance of 4.5 cm for tantalum, tungsten and stainless steel. Depending on the gas temperature of the plasma of about 230 °C the sample temperature increases to maximal 220 °C. In all

measurements the floating potential ranges between -3 to -2 V whereas the plasma potential lies between 0 to 1.5 V and an ionic flux of some $10^{19} (m^2 s)^{-1}$ is present.

With increasing distance the relative negative ion density increases linearly for tantalum, tungsten and the stainless steel reference sample. Compared to stainless steel, for tantalum and tungsten no significant variances of n_{H^-}/n_e exceeding the error margins is present reaching maximal about 13.5% at a distance of 4.5 cm (figure 3(a)). In contrast, over the complete investigated distance range an enhanced relative negative ion density is measured with the caesiated sample also showing a different dependency on the distance. At 0.5 cm a maximal value of 10.1% is reached that is 2.8 times increased compared to the stainless steel reference sample. It has to be pointed out that compared to the investigated caesiated sample a direct application of caesium onto a sample surface might result in even higher n_{H^-} .

Within a variation of the hydrogen pressure between 0.3 and 3 Pa measured at 4.5 cm distance for tantalum, tungsten and the stainless steel reference sample no significant variation between the samples is seen, showing a peaked non-monotonic evolution of n_{H^-}/n_e at 0.5 Pa figure 3(b).

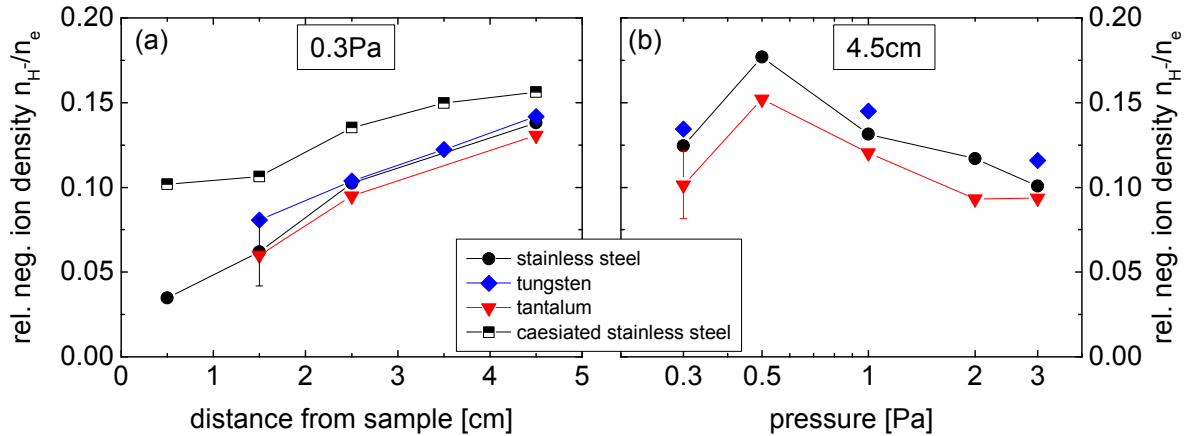


FIGURE 3. Relative negative ion density measured with floating samples of tantalum, tungsten, caesiated stainless steel and a stainless steel reference sample at a discharge power of 300 W and a sample temperature $\approx 220^\circ\text{C}$. (a) n_{H^-}/n_e at 0.3 Pa as function of the distance from the surface. (b) n_{H^-}/n_e as a function of pressure at a distance of 4.5 cm from the surface.

Variation of sample temperature

In figure 4 the effect of varying the sample temperature up to 600°C on the relative negative ion density for tantalum, tungsten and LaB_6 is shown measured at 0.3 Pa and 300 W discharge power in a distance of 4.5 cm from the samples. On the one hand these measurements are aimed at investigating an additional thermally induced cleaning effect. On the other hand, for tungsten a variation of sample temperature also is addressed on investigating the effect of thermionic emitted electrons on the negative ion density. The surface production of H^- is due to a transition of a surface electron to the hydrogen atom. Following the Richardson-law the probability for thermionic emission of electrons depends on the material work function and temperature. This process has a similarity to an oxidation process at surfaces. For tungsten a high reactivity for oxidation is known at elevated temperatures. Hence it might be possible that an increased surface temperature may also be beneficial for surface formation of negative ions. Investigations on LaB_6 are focused on using a low work function material for affecting the negative ion density. For single-crystalline LaB_6 work functions down to 2.3 eV have been measured [26].

In principle within the error margins a temperature variation in the investigated range does not reveal a significant effect on n_{H^-}/n_e for tantalum, tungsten and LaB_6 . Mean relative negative ion densities for tantalum of 11.7%, 13.5% for tungsten and 12.5% for LaB_6 are measured. However, one might interpret a slight enhancement of n_{H^-}/n_e in the case of tungsten for increasing temperature.

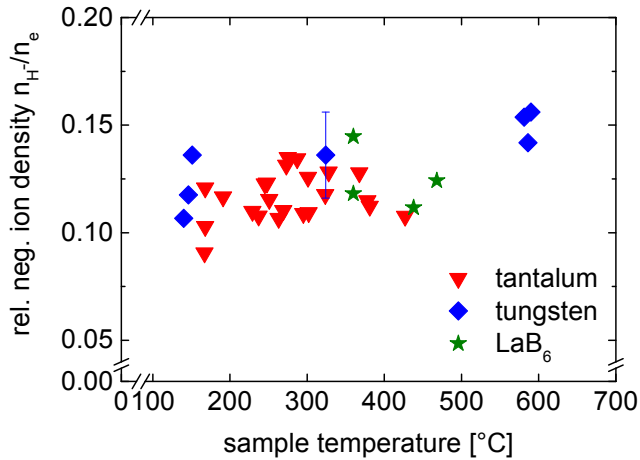


FIGURE 4. Relative negative ion density measured at a distance of 4.5 cm from the floating surfaces at 0.3 Pa and 300 W discharge power for varying temperature.

Effect of Cs-free materials on the relative negative ion density

In figure 5 the relative negative ion density for different caesium-free materials measured at a pressure of 1 Pa and 300 W discharge power in a distance of 4.5 cm from the surfaces is compared. The depicted values are averaged results of different measurements that were conducted under the same external parameters. Additionally to the measurements with tantalum, tungsten and LaB_6 , figure 5 is extended by first measurements of n_{H^-}/n_e above DLC samples. The investigations on DLC are focused on the influence of such surfaces on the negative ion density as well as on the surface stability due to hydrogen plasma exposure. For that purpose measurements were obtained after one hour plasma operation. The surface temperature during these measurement was about 220 °C. While for stainless steel, tantalum, tungsten and LaB_6 no erosion due to plasma exposure has been observed a clear impact on the DLC surface due to erosion could be seen by scanning electron microscopy. Compared to the stainless steel sample none of the materials lead to a significant enhancement of n_{H^-}/n_e , the averaged n_{H^-}/n_e is 14.3%.

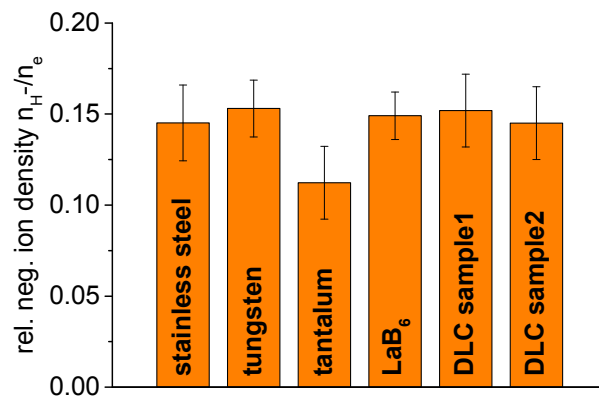


FIGURE 5. Relative negative ion density measured at a distance of 4.5 cm from different floating surfaces at 1 Pa and 300 W discharge power. The sample temperature was maximal about 220 °C.

Discussion

As a reference for pure volume formation of negative hydrogen ions the stainless steel reference sample is used. The pressure dependence of volume formation and destruction mechanisms is discussed in [23] showing that at HOMER negative ions produced via dissociative attachment are dominantly destroyed by collisions with atomic hydrogen, namely associative and non-associative detachment. It is shown that n_{H^-} is determined mainly by the pressure dependent evolution of n_e and of the population of highly vibrationally excited hydrogen molecules. Both parameters directly influence the rate of H^- volume production.

For the stainless steel reference sample the observed change of the relative negative ion density with changing distance is again attributed to a variation of volume production and destruction mechanisms. This will be further investigated by modelling and distance dependent OES.

For tantalum and tungsten the same dependency of H^- on pressure and distance variation like for the stainless steel reference sample have been measured at HOMER. On the contrary, in investigations made by [8] at a filament driven multicusp source, an enhancement of the negative ion density has been reported when metal liners made of tantalum and tungsten were used instead of stainless steel. They proposed that this might be an inherent characteristic of filament driven sources related to a material dependent secondary electron emission that is induced by high energetic primary electrons. The effect of tantalum also has been investigated at the Camembert III test bed operated as a filament and as an ECR-driven source [11, 27]. An increased negative ion yield is reported when the stainless steel walls were modified by evaporating tantalum filaments. The observed effect has been explained by the production of vibrationally excited molecules due to recombinative desorption at the walls. When Camembert III was operated as an ECR-discharge a time dependent decrease of the measured n_{H^-} has been observed and explained by a possible change of the wall surface that was recoverable by evaporation of fresh tantalum. However, in a third experimental setup, an ECR-driven ion source where the tandem principle is applied by the meshed grid method, a change of the grid material from stainless steel to tantalum has resulted in a reduced extracted negative ion current [18].

These different results indicate that in an ECR-discharge where no high energetic primary electrons are present, no enhancing effect on the negative ion density is given due to bulk materials of tantalum or tungsten and confirm the measurements performed at HOMER.

At HOMER elevated temperatures of the samples had no effect on the measured negative ion density. This can be due to several effects. A coverage of the samples with impurities seems unlikely as with increasing temperature a thereby induced cleaning had no effect on the negative ion density. For tungsten measurements with elevated temperatures up to 850 K also were focused on the effect of thermionic emitted electrons on n_{H^-} . Known from the Richardson-law for thermionic emission a temperature of about 810 K is needed for providing the same emitted current for a material having a work function of 4.5 eV compared to a material at 400 K and a work function of 2.2 eV. However, if negative ion formation can be induced by this method it might be possible that even higher temperatures than the investigated ones are needed for affecting the negative ion density. At the present measurements no significant enhancement on the negative ion density has been obtained.

For the investigated LaB_6 sample no effect on the negative ion density has been observed for temperatures up to $T_{\max} \approx 450^\circ\text{C}$. This might be related to the work function of the investigated sample. However, the work function of this polycrystalline sample is not known at present. Hence, further measurements are needed and will be conducted at ACCesS. It has to be pointed out that the absence of an effect on the negative ion density again also might be related to the low temperatures applied in the present investigations.

First measurements conducted with two DLC samples of different surface roughness have shown a diverse time dependent evolution in the measured relative negative ion density during plasma operation. In the case of a rough surface structure a decreasing n_{H^-}/n_e is measured over time. In contrast, for the sample having a smooth surface the relative negative ion density is increasing. After 50 minutes hydrogen plasma exposure the measured relative negative ion densities determined for both samples are comparable indicating an equalisation of the surface structure due to erosion. Compared to the pristine samples the surfaces clearly are affected by plasma exposure. This is confirmed by scanning electron microscopy where a changed surface roughness can be seen.

In conclusion, compared to the stainless steel reference sample for none of the investigated caesium-free materials an enhancement of the negative ion density in the plasma volume has been observed at HOMER. However, due to a caesiated stainless steel sample the negative ion density increases, confirming the surface production of negative ions at caesiated surfaces. This shows that at HOMER a surface induced effect on the negative ion density only can be observed when the surface effect exceeds the present volume production of negative hydrogen ions. This is realistic for negative hydrogen ion sources and beneficial for evaluating a materials potential for being a caesium-free alternative for efficient negative hydrogen ion formation.

CONCLUSION AND OUTLOOK

Caesium-free alternatives for efficient negative ion formation under ion source relevant parameters are investigated. By means of laser photodetachment the effect of different materials on the relative negative ion density is measured. The tandem principle is applied by the usage of a meshed grid. Due to the meshed grid conditions are provided where negative ions are efficiently formed by volume processes at significantly lowered electron densities. Downstream of the meshed grid the effect on the negative ion density due to tantalum, tungsten, LaB₆, two types of DLC and a caesiated stainless steel sample have been measured and compared to a stainless steel reference sample. Enhanced negative ion densities have been measured due to the caesiated stainless steel sample confirming the surface production of negative ions at caesiated surfaces. However, for the caesium-free materials no significant enhancement of the negative ion density has been obtained under the plasma conditions being present at HOMER. Elevated surface temperatures investigated for tantalum, tungsten and LaB₆ showed no dependency of n_{H^-}/n_e on this parameter. In first investigations on DLC a clear erosion due to hydrogen plasma exposure has been observed. Further investigations regarding, among others, the crystalline structure of the samples are necessary for evaluating the potential of these materials for efficient negative ion formation at negative ion sources. The present investigations show that at HOMER the effect of a material on the negative ion density only is observed when it exceeds the present volume formation process. This also is mandatory for suitable materials for efficient H⁻ formation in negative hydrogen ion sources. It is scheduled to extend the present investigations on materials for which negative ion surface formation has been reported like highly ordered pyrolytic graphites (HOPG) and different diamond samples [14].

ACKNOWLEDGMENTS

This work has been carried out within the framework of the EUROfusion Consortium and has received funding from the European Union's Horizon 2020 research and innovation programme under grant agreement number 633053. The views and opinions expressed herein do not necessarily reflect those of the European Commission.

REFERENCES

1. Belchenko, Y.I. et al., *Nucl. Fusion* **14**, 113 (1974).
2. Lee, B.S. et al., *Appl. Phys. Letters* **61**, 2857–2859 (1992).
3. Speth, E. et al., *Nucl. Fusion* **46**, S220 (2006).
4. Fantz, U. et al., *Chem. Phys.* **398**, 7 – 16 (2012).
5. Wurz, P. et al., *Surf. Science* **373**, 56 – 66 (1997).
6. Goeden, C. et al., *Diam. Rel. Mat.* **9**, 1164 – 1166 (2000).
7. Scheer, J.A. et al., *Nucl. Instr. Phys. Res. Sec. B: Beam Interactions with Materials and Atoms* **230**, 330 – 339 (2005).
8. Leung, K.N. et al., *Appl. Phys. Letters* **47**, 227–228 (1985).
9. Inoue, T. et al., *Plasma Sources Sci. Technol.* **1**, 75 (1992).
10. Fukumasa, O. et al., *J. Phys. D: Appl. Phys.* **20**, 237 (1987).
11. Bacal, M. et al., *Rev. Sci. Instr.* **75**, 1699–1703 (2004).
12. Schiesko, L. et al., *Plasma Sources Sci. Technol.* **19**, 045016 (2010).
13. Kumar, P. et al., *J. Phys. D: Appl. Phys.* **44**, 372002 (2011).
14. Ahmad, A. et al., *J. Phys. D: Appl. Phys.* **47**, 085201 (2014).
15. Hall, R.I. et al., *Phys. Rev. Lett.* **60**, 337–340 (1988).
16. Čadež, I. et al., *Zeits. f. Phys. D Atoms, Molecules and Clusters* **26**, 328–330 (1993).
17. Schermann, C. et al., *The Journal of Chem. Phys.* **101**, 8152–8158 (1994).
18. Gobin, R. et al., *AIP Conf. Proc.* **763**, 289–295 (2005).
19. Lienemann, J. et al., *Nucl. Instr. Phys. Res. Sec. B: Beam Interactions with Materials and Atoms* **269**, 915 – 918 (2011).
20. Schiesko, L. et al., *Plasma Sources Sci. Technol.* **17**, 035023 (2008).
21. Fukumasa, O. et al., *AIP Conf. Proc.* **287**, 411–421 (1992).
22. Bacal, M. et al., *Rev. Sci. Instr.* **50**, 719–721 (1979).
23. Rauner, R. et al., *Contribution to these proceedings* (2014).
24. Fantz, U., *Contrib. Plasma Phys.* **44**, 508–515 (2004).
25. Friedl, R. et al., *Contribution to these proceedings* (2014).
26. Yamauchi, H. et al., *Appl. Phys. Letters* **29**, 638–640 (1976).
27. Bacal, M. et al., “ECR-Driven Multicusp Volume H- Ion Source,” 2005, vol. 763, pp. 203–213.